Journal of Materials Chemistry A

Accepted Manuscript

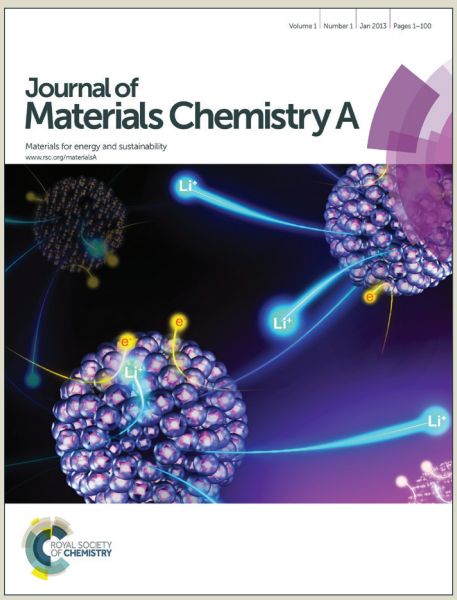

ROYAL SOCIETY OF CHEMISTRY

www.rsc.org/materialsA

Investigation on the adsorption properties of Cr(VI) ions on a novel graphene oxide (GO) based composite adsorbent

Jian Hua Chen[1, 2, *], Hai Tao Xing[1], Hong Xu Guo[1], WenWeng[1, 2], Shi Rong Hu[1], Shunxing Li[1, 2], Yi Hong Huang[1], Sun xue[1], Su zhen Bo[1]

1. College of Chemistry and Environmental, Minnan Normal University, Zhangzhou 363000, China
2. Fujian Province University Key Laboratory of Modern Analytical Science and Separation Technology, Minnan Normal University, Zhangzhou 363000, China

Abstract

In this study, we prepared polyethyleneimine (PEI) and graphene oxide (GO) composite adsorbent PEI-GO through an amidation reaction between the amine groups of the PEI and the carboxyl groups of the GO. Adsorption performance of the PEI-GO was tested by removing Cr(VI) ions from an aqueous solution. The physico-chemical properties of the GO, pristine and Cr(VI) ions loaded PEI-GO were investigated by the FT-IR, SEM-EDX and XPS methods. To investigate the adsorption kinetics of Cr(VI) ions onto this newly developed PEI-GO, we performed a batch of experiments under different adsorption conditions: content of the PEI in the PEI-GO, solution pH, initial Cr(VI) ion concentration, adsorption temperature and contact time. The prepared PEI-GO exhibited an encouraging uptake capacity of 539.53 mg/g. The adsorption process was fast, within the first 1 h, Cr(VI) ion adsorption onto the PEI-GO was about 71 %, and the adsorption equilibrium could be obtained within 14 h. Kinetics experiments indicated that the adsorption process could

* Corresponding author: Chen JH, e-mail: jhchen73@126.com; Phone: 86-596-2591445; Fax: 86-596-2520035

be described by the pseudo-second-order kinetic model. Furthermore, our adsorption equilibrium data fit the Langmuir isotherms well (R^2>0.99). The removal mechanism of Cr(VI) ions from the solution consists of two steps: (1) Cr(VI) ions binds to the 4PEI-GO by the electrostatic interaction between the negatively charged Cr(VI) ions species and the protonated amine groups of the 4PEI-GO; and (2) small part of Cr(VI) ions were reduced to Cr(III) ions with the assistance of π electrons on the carbocyclic six-membered ring of the 4PEI-GO and then bind on the 4PEI-GO by the electrostatic attraction between Cr(III) ions and negatively charged groups (COO^-) of the 4PEI-GO. Based on the results obtained in this work, it can be concluded that the prepared PEI-GO can be an effective and potential adsorbent for removing Cr(VI) ions from an aqueous solution.

Key word: Graphene oxide (GO); Polyethyleneimine (PEI); Adsorption; Cr(VI)

Introduction

In aqueous systems, chromium usually exists in both trivalent and hexavalent oxidation states, but they were significantly difference between the toxicity. Cr(III) is essential to animals and plants and plays an important role in sugar and fat metabolism in low concentration[1], whereas Cr(VI) is more toxic than Cr(III) because it is extremely mobile in the environment and very toxic and carcinogenic to living organism[2,3]. It can cause liver damage, pulmonary congestions, and severe diarrhea. Even in low concentrations, Cr(VI) can also cause harm to human body, due to their bioaccumulation through the food chain and hence in the human body. Actually, the discharge limit of Cr(VI) was restricted to be only 0.05 $mg.L^{-1}$ by the US Environmental Protection Agency (EPA). A lot of industrial wastewaters contain Cr(VI), such as leather tanning, mining of chrome ore, alloys dyes and pigment manufacturing, etc[4-7]. To avoid the adverse biological and ecological impacts of Cr(VI) pollution, it must be substantially removed from the wastewater before being discharged into the aquatic system. The development of methods for effective removing Cr(VI) from wastewater is an important task for healthy living. A number of technologies to remove Cr(VI) have been developed, including electro-chemical precipitation[8,9], reverse osmosis[10,11], ion exchange[12,13] and adsorption[14-20]. Among the above methods, adsorption has become by far the most versatile and widely used technology. The main advantages of the adsorption are recovery of the heavy metal, less sludge volume produced, simplicity of design and the meeting of strict discharge specification. Several adsorbents that have been studied for Cr(VI) removal include

activated carbon[21,22], inorganic materials[23,24] and biosorbents[25-28]. However, these adsorbents have been suffering from either low adsorption capacity or low efficiency. As a result, it is highly desirable to develop new adsorbent materials with large surface area, high adsorption capacity and stability in extreme conditions.

Nowadays, nanomaterials have gradually playing an important role in wastewater treatment[29-31]. The benefits from the use of nanomaterials for metal removal may derive from their enhanced reactivity and high specific surface area. Graphene-based composites[32-37]are one type of these materials that have potential applications in the wastewater treatment system. Among the graphene-based adsorbents, graphene oxide (GO) shows the promising performance in treating heavy metal ions and cationic dyes[38-40]. The oxidation process of graphite to graphene oxide can introduce abundant functional groups on the GO surface, such as –COOH, –C=O and –OH. These groups are the essential reactive functional groups for an ideal adsorbent[41-46]. However, due to the well disperses of the GO in water, the separation of the GO after adsorption is very difficult, therefore, high speed centrifugation is required. Obviously, that is unpractical for water treatment due to the large quantity of wastewater. Another drawback of the GO adsorbent is that it usually suffers from serious agglomeration and restacking during utilization due to the π–π interactions between neighboring sheets, which leading to a great loss of effective surface area and consequently a lower adsorption capacity than expected[47-49]. Polyethyleneimine (PEI) is a kind of water-soluble polyamine and is well known for its metal chelation properties due to a large number of primary and secondary amine groups presenting in the molecule[28,50].

In previous studies, some researchers coat the PEI on the surface of ion exchange resin or silica gel particles to adsorption separation heavy metals from water system [51], but the adsorption efficiency is not ideal.

Due to lots of oxygen functional groups on their basal planes and edges, the GO could show high affinity to amines or amine-containing molecules. If the PEI polymers are attached to substrate (GO), it can effectively reduce or prevent the restacking and agglomeration of the GO nanosheets. Meanwhile, the residual amine groups of the PEI can also exhibit good adsorption capacity for polyanions and negatively charged organic or inorganic. As we all known, at low pH, Cr(VI) exists as negatively charged ions[52]. Therefore, the PEI-GO composite may be an effective adsorbent for removing of Cr(VI) ions from wastewater. Based on the mention above, in this study, a composite adsorbent PEI-GO was prepared. To investigate the factors that affect the adsorption capacity of the PEI-GO for Cr(VI) ions, we carried out a batch of adsorption experiments under various conditions: content of the PEI in the PEI-GO, solution pH, adsorption temperature, initial Cr(VI) ion concentration and contact time. By testing various adsorption and kinetics models to fit our experimental data, we also studied the adsorption kinetics, isotherms and adsorption mechanism of the PEI-GO composite material for Cr(VI) ions.

Experimental section

Material

Natural flake graphite was purchased from Qingdao Hengsheng graphite Co. Ltd. Potassium dichromate ($K_2Cr_2O_7$%≥99.8, Xilong Chemical Co. Ltd., China).

1-ethyl-3-(3-dimethylaminoprophy) carbondiimide hydrochloride (EDC·HCl), N-hydroxyl succinimide (NHS), branched polyethylenimine (M.W.70000, 50% in water) were obtained from Aladdin. Other chemicals of analytical grade were obtained from the China National Medicine Corporation and used as received. A stock solution of 1000 $mg.L^{-1}$ of Cr(VI) ions was prepared by dissolving $K_2Cr_2O_7$ in deionized water. The desired Cr(VI) ion solution were prepared by diluting of the stock Cr(VI) ion solution. Solutions of 0.1 M NaOH and 0.1 M HCl were used for adjusting the solution pH.

Synthesis of the GO

The GO was synthesized from natural flake graphite by modified Hummers method[53,54]. In briefly, 5.0 g of graphite powder was mixed with 150 mL concentrated H_2SO_4 and 8.0 g $NaNO_3$ at 273 K. Maintaining vigorous stirring, 20.0 g of $KMnO_4$ was added gradually and the temperature of the mixture was controlled at 277 K. The reaction mixture was stirred at 308 K for 2 h until it became pasty brownish, and diluted with 150 mL of deionized water. Then, 50 mL of 30 wt. % H_2O_2 was slowly added to reduce the residual $KMnO_4$, after which the color of the mixture changed to brilliant yellow. The resultant mixture was filtered and washed with 5 wt. % HCl aqueous solution and deionized water. For further purification, the as-obtained GO was re-dispersed in deionized water and then was dialyzed for one week to remove residual salts and acids.

Synthesis of the PEI-GO composites

The produce of preparing of the PEI-GO composites (in this reaction process

(Scheme.1 ESI†), we synthesized PEI-GO composites with different PEI content): 0.3 g of the as-obtained GO was dispersed in 100 mL of deionized water and sonicated for 0.5 h. Then, a certain amount of PEI (the mass of PEI was mentioned in the section of "Optimization of the PEI loading on the GO"), 0.45 g of EDC·HCl and 0.24 g of NHS was added. The pH of the resultant solution was maintained at 7.0. After reaction for 24 h at room temperature (298 K), the solution was centrifuged and the residue was washed with deionized water for several times. The resultant products were dried in an oven at 333 K for 24 h, and stored in a desiccator for further experiments.

Batch adsorption experiments

To perform an adsorption isotherm analysis, adsorption experiments were carried out by adding 0.01 g of PEI-GO to a 100 mL of Cr(VI) solution (in 250 mL conical flasks) at room temperature (298 K). The initial Cr(VI) concentrations varied from 10 $mg.L^{-1}$ to 400 $mg.L^{-1}$, and the pH of Cr(VI) solutions was maintained at 2.0 with 0.1 M HCl or 0.1 M NaOH solutions. After adding PEI-GO, the conical flasks with solution were shaken at 120 rpm in a thermostatic shaker for enough reaction time to achieve the adsorption equilibrium. Then, the mixtures were filtered through a 0.2 μm pore size membrane. Total concentrations of chromium and Cr(VI) ions in aqueous samples were determined on a spectrophotometer at 540 nm using diphenyl carbazide as the complexing agent. The relationship between total chromium and Cr(VI) ions under different initial Cr(VI) ions concentration during adsorption, as shown in the Fig. S1 ESI†. All the experiment results were an average of five replicate tests.

The adsorption capacity (q_e, $mg.g^{-1}$) of the Cr(VI) adsorbed onto adsorbent was obtained from the following equation:

$$q_e = (C_0 - C_e)v / m \qquad (1)$$

where V is the volume of the solution (L), m is the weight of the adsorbent (g), C_0 and C_e are the concentrations of Cr(VI) ions in the initial aqueous solution and equilibrium solution, respectively.

The effect of solution pH on Cr(VI) adsorption were measured using the same procedure mentioned above. In briefly, 0.01 g of the PEI-GO was added into 100 mL of 90 $mg.L^{-1}$ Cr(VI) solution with pH ranging from 2.0 to 7.0 at 298 K. The effect of temperature on the adsorption of Cr(VI) by the PEI-GO was also conducted at the temperature of the solution ranging from 298 to 328 K.

For the adsorption kinetic studies, 0.02 g of the PEI-GO was added into 200 mL of 90 $mg.L^{-1}$ Cr(VI) with a contact time ranging from 0 h 14 h at solution pH of 2.0. The samples were taken for Cr(VI) concentration measurements at specific time intervals. The successive adsorption−desorption studies were also carried out (Fig. S2 ESI†).

Statistical analysis

All the experiments data presented are an average of five replicate tests at the same initial concentration from independent experiments and the relative error was less than 5%. Standard deviation is indicated wherever necessary. More information about the statistical analysis can be available in Electronic supplementary information (ESI†).

Results and discussion

Optimization of the PEI loading on the GO

The amount of PEI anchored on the surface of the GO is a key factor in determining the adsorption capacity of Cr(VI) by the PEI-GO. On the one hand, higher loadings of the PEI will enhance the adsorption properties of the PEI-GO for Cr(VI). On the other hand, too high loading of the PEI will decrease the exposed adsorptive sites of the PEI-GO for Cr(VI), thus resulting in a lower adsorption capacity. Therefore, it is necessary to optimize the loading of PEI in the PEI-GO. In this work, the PEI-GO composites with different PEI loadings were prepared by simply varying the amount of the PEI (2.0 g, 3.0 g, 4.0 g, 5.0 g, 6.0 g) while kept the amount of the GO (0.3 g) unchanged. The resultant composites were denoted as 2PEI-GO, 3PEI-GO, 4PEI-GO, 5PEI-GO and 6PEI-GO, respectively. **Fig. 1** shows the effect of the PEI content on adsorption capacity of the PEI-GO for Cr(VI). The results proved that Cr(VI) adsorption capacity of the GO was greatly enhanced by modifying with the PEI. It was also found that the adsorption ability increased from the 2PEI-GO to 4PEI-GO. This can be attributed to the increase in the chelation sites of the PEI-GO due to the increasing content of the PEI in the PEI-GO. However, comparing the 5PEI-GO and 6PEI-GO with the 4PEI-GO, we could found there was a decrease in adsorption capacity. This decrease might be attributed to that too much surface of the GO covered by the PEI decreased the exposed adsorptive site of the GO for Cr(VI) and hence the adsorption capacity of the GO for Cr(VI). Therefore, we chose the 4PEI-GO as a model for further investigation.

Characterization of the 4PEI-GO

The FT-IR spectra of the GO and 4PEI-GO are shown in **Fig. 2**. The characteristic peaks of the GO (**Fig. 2a**) appear at 1723 cm^{-1} (C=O in carboxyl group), 1622 cm^{-1} (C=C in the aromatic ring), 1387 cm^{-1} (C-OH group) and 1066 cm^{-1} (C-O-C in the epoxide group), respectively. While in the FT-IR spectrum of the 4PEI-GO (**Fig. 2b**), there are two characteristic absorbance bands centered at 1658 cm^{-1} and 1522 cm^{-1}, which correspond to the C=O stretching vibration of -NHCO- and the N-H bending of $-NH_2$, respectively. The FT-IR result proves that $-NH_2$ groups on the PEI have been reacted with the -COOH groups of the GO.

The SEM images of the GO, pristine and Cr(VI) ions loaded 4PEI-GO are shown in **Fig. 3** (a), (b) and (c), respectively. The GO presents the sheet-like structure with smooth surface and wrinkled edge. After the combination with the PEI to form the 4PEI-GO composite, the 4PEI-GO had a much rougher surface, revealing that the PEI had been assembled on the surface of the GO layers with a high density. After the reaction of Cr(VI) ions with the 4PEI-GO, the surface morphology of the 4PEI-GO has changed significantly, indicating that a mass of Cr(VI) has been loaded on the surface of the 4PEI-GO.

Influence of solution pH

The relation between the initial pH of solution and the adsorption capacity of Cr(VI) is shown in **Fig. 4**. It was found that a higher adsorption capacity was obtained at a lower solution pH. The effect of solution pH can be explained by the surface charge of the adsorbent and the degree of ionization of the adsorbate. It is well known that

Cr(VI) ions exists in various anionic forms (i.e., $H_2Cr_2O_7$, $Cr_2O_7^{2-}$, $HCrO_4^-$, CrO_4^{2-} and $HCr_2O_7^-$) in aqueous solution, depending on the solution pH and concentration[55,56]. H_2CrO_4 exists mainly at solution pH less than about 2.0; -$HCrO_4^-$ and -$Cr_2O_7^{2-}$ were usually found in the solution pH range of 2.0-6.0, and when the solution pH increases to above 7.0, CrO_4^{2-}will be the primary form[52]. So when the solution pH is changed, the existed form of Cr(VI) ions will influence the uptake capacity of the 4PEI-GO for Cr(VI). The surface of the 4PEI-GO is covered with amino groups that vary in form at different pH levels. Under strong acidic conditions, amino groups will be protonated to form the positively charged sites (such as -NH_3^+) and result in the electrostatic attraction with the negatively charged Cr(VI) ions[37,55-56], leading to the increase of removal efficiency. With an increasing in solution pH, the ability of -NH_2 to be protonated weakened, and at the same time the concentration of OH^- increased and competed with anionic Cr(VI) ions, which resulted in a decline of Cr(VI) ions remove efficiency. Thus, pH of 2.0 was selected as the optimum pH value of Cr(VI) solution for the following adsorption experiment.

Influence of solution temperature

The effects of temperature on the adsorption capacity of the 4PEI-GO for Cr(VI) ions are presented in **Fig. 5**. The increase in Cr(VI) adsorption capacity of the 4PEI-GO with increasing temperature indicated the endothermic nature of the adsorption process. To investigate the mechanism involved in the adsorption, the thermodynamic behaviour of Cr(VI) ion adsorption onto the 4PEI-GO were evaluated by the following equations:

$$\ln(q_e / \boldsymbol{C}_e) = -\Delta H / RT + \Delta S / R \quad (2)$$

$$\Delta G = \Delta H - T\Delta S \quad (3)$$

R is the universal gas constant (8.314 J mol^{-1} K^{-1}) and ***T*** is the absolute temperature (in Kelvin). Plotting $\ln(q_e/C_e)$ against 1000/T gives a straight line with slope and intercept equal to −ΔH/R and ΔS/R, respectively. It is described in **Fig. 6**. Thermodynamic parameters are calculated according to **Eqs.(2)-(3)** shown in **Table1**. The negative ΔG indicate that the adsorption process is spontaneous. These values decreased with an increase of temperature indicating a better adsorption performance was obtained at higher temperature. The positive value of ΔH confirms the endothermic nature of the overall adsorption process and positive value of ΔS suggests an increasing randomness at the solid/solution interface during the adsorption process.

Adsorption isotherm

An adsorption isotherm expresses the relationship between the amount of adsorbate adsorbed per unit weight of adsorbent (q_e, $mg.g^{-1}$) and the concentrations of adsorbate in the bulk solution ($\boldsymbol{C}_e$, $mg.L^{-1}$) at a given temperature under equilibrium conditions. Adsorption isotherm gives important information about the mechanism of adsorption and helps us in the design of new adsorbing systems. To determine the parameters associated with Cr(VI) adsorption, the experimental data are analyzed using the Langmuir and Freundlich adsorption isotherm models, respectively. The Langmuir model assumes uniform energies of adsorptive site on the surface of adsorbent and no transmigration of adsorbate in the plane of the surface. It can be expressed as Eq. (4)

$$C_e / q_e = C_e / q_{max} + 1/(q_{max} k_1) \quad (4)$$

The Freundlich isotherm is empirical isotherm can be used for non-ideal adsorption that is multilayer adsorption. The Freundlich isotherm is represented by the following Eq. (5)

$$\lg q_e = \lg k_f + (1/n)\lg C_e \quad (5)$$

where q_e is the adsorption amount of Cr(VI) on adsorbent ($mg.g^{-1}$) at an equilibrium state, q_{max} is the maximum adsorption capacity of metals on adsorbent ($mg.g^{-1}$), C_e is the equilibrium concentration of metals ($mg.g^{-1}$), and k_1 is the Langmuir adsorption constant, which is related to the adsorption energy. k_f and n are Freundlich constants related to adsorption capacity and adsorption intensity, respectively.

From **Fig. 7**, we can find that Cr(VI) ions are favorably adsorbed on the 4PEI-GO and the adsorption capacity of Cr(VI) attained 539.53 $mg.g^{-1}$ at an equilibrium concentration of 294.72 $mg.L^{-1}$, The adsorption capacity obtained with the 4PEI-GO is much higher than those obtained with many other adsorbents, as shown in **Table2.**

A linear fitting was applied to obtain the Langmuir and Freundlich isotherms parameters (as shown in **Fig. 8)** and the relevant parameters are presented in **Table3**. Taking into consideration the values of the correlation coefficient as a criterion for goodness of fitness for the system, the Langmuir model shows better correlation (R^2=0.994) than the Freundlich model(R^2=0.992), which indicates that the Langmuir equation represented the adsorption process more ideally.

In addition, EDX can be used to track the adsorption process through the analysis of the surface element contents. As shown in **Fig. 9**, the signal of Cr observed at the

4PEI-GO and GO surface indicates that Cr has been adsorbed onto the 4PEI-GO and GO surface. Obviously, the signal strength of Cr appeared at the 4PEI-GO surface are stronger than that of at the GO surface, the results has also suggest that the PEI can dramatically increase the adsorption capacity of the heavy metals.

Adsorption kinetics study

Fig. 10 shows the adorption kinetic of chromium at room temperature (298 K) with Cr(VI) concentrations of 90 $mg.L^{-1}$. The kinetic data were analyzed using pseudo-second order kinetics[48], and can be expressed as follows:

$$t / q_t = 1 / v_o + t / q_e \quad (6)$$

$$v_o = k_2 q_e^{\ 2} \quad (7)$$

where q_e is the adsorption capacity ($mg\ g^{-1}$) at equilibrium, q_t is the loading of Cr(VI) at time t, v_o is the initial adsorption rate ($mg.g^{-1}.min^{-1}$), and k_2 ($mL.mg^{-1}.min^{-1}$) represent the pseudo-second-order rate constant for the kinetic model. The slope and intercept of the linear plot of t/q_t against t yield the values of q_e and k_2 as shown in **Fig. 11**. The fitting results obtained from the models are summarized in **Table4**. The correlation coefficient (R^2) was relatively high (>0.99), and the calculated q_e values from the model fitting were very close to the experimental ones. These results imply that the overall rate of the adsorption process is controlled by chemisorption.

Selective adsorption and real water sample experiment

It is more important to evaluate the simultaneous adsorption behavior and interactions involving two or more metal species since sole toxic metal species rarely exist in natural streams and waste effluents. For the selective adsorption experiment, we used

the Ni(II), Cu(II), Cd(II) as the coexisting metal ions. A 0.01 g of 4PEI-GO was dispersed in a 100 mL mixed solution, which contained Cr(VI), Ni(II), Cu(II) and Cd(II). The initial concentration of each metal ion was 200 $mg.L^{-1}$, and the pH of the solution was 2.0, the mixture was stirred for enough time at 298 K. After adsorption, the mixture was filtered through a 0.2 μm membrane and the filtrate was tested for different metal ions. **Fig. 12** shows the effects of coexisting metal ions on Cr(VI) adsorption. The results indicated that the Cr(VI) adsorption performance was slightly decreased due to the presence of Ni(II), Cu(II), Cd(II) ions in the solution. This observation may be explained by the decrease in the number of binding site on the 4PEI-GO because co-existing ions compete with Cr(VI) for adsorption. However, the 4PEI-GO has much higher Cr(VI) selectivity than the Ni(II), Cd(II), Cu(II) ions in the solution. For the real water matrix experiment, the electroplating wastewater (Zhangzhou electroplating factory) spiked with 11.0$mg.L^{-1}$ Cr(VI) was used to evaluate practical application of 4PEI-GO. **Table5** shows the initial concentration and the removal efficiencies of Cr(VI) after treatment with 4PEI-GO. For the studied water samples, the observed removals of Cr(VI) were 96.4% and were hardly influenced by the commonly coexisted ions in electroplating wastewater. Compared with the removal percentage abstained from **Fig. 7**, it is evident that coexisted ions in electroplating wastewater have weak influence on the removal efficiency of Cr(VI) with 4PEI-GO.

Adsorption mechanism

To investigate the main mechanism of Cr(VI) removal, it is very important to

ascertain the oxidation state of the chromium bound on the 4PEI-GO. The valence state of chromium bound to the 4PEI-GO was confirmed by XPS analysis. The high resolution XPS spectrum (**Fig. 13**) of the Cr 2p region can be curve-fitted with four components at binding energies of 579.3 eV, 581.2 eV, 589.3eV and 590.2 eV. The peak located at 579.3 eV and 581.2 eV correspond to Cr $2p_{3/2}$ orbitals, while those appeared at 589.3 eV and 590.2 eV correspond to Cr $2p_{1/2}$ orbitals. The peaks at binding energies of 579.3 eV and 589.3 eV can be attributed to Cr(III) while the peaks at 581.2 and 590.2 eV can be regarded as the signals of Cr(VI)[66]. These results indicate that both Cr(VI) and Cr(III) coexist on the 4PEI-GO. Therefore, it can be speculated that the removal mechanism consists of two steps: (1) Cr(VI) binds to the 4PEI-GO by the electrostatic interaction between the negatively charged Cr(VI) species and the protonated amine groups of the 4PEI-GO; and (2) small part of Cr(VI) is reduced to Cr(III) with the assistance of π electrons on the carbocyclic six-membered ring of the 4PEI-GO and then bind on the 4PEI-GO by the electrostatic attraction between Cr(III) and negatively charged groups (COO^-) of the 4PEI-GO. For the practical application of 4PEI-GO, we also consider possible effects of other cations that can be present in waste water streams. As can be seen from the **Fig. 12**, under the optimal conditions, the adsorption performance of 4PEI-GO for Cr(VI) was significantly higher than that for other coexisting metal cations, this may be associated with the strong coordination ability of 4PEI-GO for Cr(VI) ions

Conclusion

In this study, a novel graphene-based composite adsorbent (4PEI-GO) has been

synthesized through amidation reaction between the amine groups of the PEI with the carboxyl groups of the GO. Some important parameters that affected the adsorption behavior of the 4PEI-GO for Cr(VI) ions from aqueous solutions were also tested. The adsorption capacity of the 4PEI-GO for Cr(VI) ions were significantly higher than that of the pure GO. The adsorption capacity of the 4PEI-GO for Cr(VI) ions was high pH-dependent, and the adsorption capacity of the 4PEI-GO for Cr(VI) ions decreased with an increasing of solution pH. Adsorption capacity of the 4PEI-GO for Cr(VI) ions was also temperature-dependent, an increasing of temperature enhanced adsorption capacity of the 4PEI-GO. Under the present experiment condition, the maximum uptake capacity of the 4PEI-GO for Cr(VI) ions under the optimal condition was 539.53 $mg.g^{-1}$, which was significantly higher than that of other conventional adsorbents, such as ethylenediamine-functionalized Fe_3O_4, PVP modified activated carbon, mesoporous TiO_2, polypyrrole/Fe_3O_4 nanocomposite, hierarchical porous carbon, chitosan–Fe(III) complex, as shown in **Table2**. The kinetics adsorption data could be well fitted with pseudo-second-order kinetic model, and the equilibrium data can be well fitted with the Langmuir model. Based on the experiment results, the prepared 4PEI-GO can be promising adsorbent for removing Cr(VI) ions from an aqueous solution with high efficiency.

Acknowledgements

The authors would like to acknowledge the financial support of this work from National Natural Science Foundation of China (No. 21076174), National Natural Science Foundation of China (No. 21175115), Outstanding Youth Science Foundation

of Fujian Province of China (No.2012J06005), and the Science and Technology keyProject of Fujian (2013H0053). The authors also thank the anonymous referees for comments on this manuscript.

References

1 J. Kotas and Z. Stasicka, *Environ. Pollut*., 2000, **107**, 263.

2 P. Miretzky and A.F. Cirelli, *J. Hazard. Mater*., 2010, **180**, 1.

3 D. Mohan, S. Rajput, V.K. Singh, P.H. Steele and C.U. Pittman Jr, *J. Hazard. Mater*., 2011, **188**, 319.

4 V. Sarin, T.S. Singh and K.K. Pant, *Bioresour. Techonol*., 2006, **97**, 1986.

5 R. Kumar, N.R. Bishnoi and G.K. Bishnoi, *Chem. Eng. J*., 2008, **135**, 202.

6 F. Venditti, A. Ceglie, G. Palazzo, G. Colafemmina and F. Lopez, *J. Colloid. Interface Sci*., 2007, **310**, 353.

7 E. Malkoc and Y. Nuhoglu, *Sep. Purif. Technol*., 2007, **54**, 291.

8 M. Uysal and A. Irfan, *J. Hazard. Mater*., 2007, **149**, 482.

9 N. Kongsricharoern and C. Polprasert, *Water Sci. Technol*., 1996, **34**, 109.

10 A. Hafez and S. El-Mariharawy, *Desalination.*, 2004, **165**, 141.

11 R.K. Goyal, N.S. Jayakumar and M.A. Hashim, *J. Hazard. Mater*., 2011, **195**, 383.

12 S. Rengaraj, C.K. Joo, Y. Kim and J. Yi, *J. Hazard. Mater*., 2003, **102,** 257.

13 S. Edebali and E. Pehlivan, *Chem. Eng. J*., 2010, **161**, 161.

14 D. Zhang, S. Wei, C. Kaila, X. Su, J. Wu, A.B. Karki, D.P. Young and Z. Guo, *Nanoscale.*, 2010, **2**, 917.

15 J.L. Wang, X.M. Zhang and Q. Yi, *J. Environ. Sci. Health A*., 2000, **35**, 1211.

16 Y.C. Sharma, B. Singh, A. Agrawal and C.H. Weng, *J. Hazard. Mater*., 2008, **151**, 789.

17 Y.A. AydIn and N.D. Aksoy, *Chem. Eng. J*., 2009, **151**, 188.

18 Y. Zhao, J.R. Peralta-Videa, J.R. Lopez-Moreno, M. Ren, G. Saupe and J. L. Gardea-Torresdey,

Environ. Sci. Technol., 2011, **45**, 1082.

19 G. Bayramoglu, M.Y. Arica, *J. Hazard. Mater.,* 2011, **187**, 213.

20 H.-D. Choi, W.-S. Jung, J.-M. Cho, B.-G. Ryu, J.-S. Yang and K. Baek, *J. Hazard. Mater.,* 2009, **166**, 642.

21 M.M. Rao, D.K. Ramana, K. Seshaiah, M.C. Wang and S.W.C. Chien, *J. Hazard. Mater.,* 2009, **166**, 1006.

22 S. Liu, J. Sun and Z. Huang, *J. Hazard. Mater.,* 2010, **173**, 377.

23 G.B. Cai, G.X. Zhao, X.K. Wang and S.H. Yu, *J. Phys. Chem. C*., 2010, 1**14**, 12948.

24 F. Fu, H. Zeng, Q. Cai, R. Qiu, J. Yu and Y. Xiong, *Chemospher.*, 2007, **69**, 1783.

25 D. Park, Y.S. Yun, J.H. Jo and J.M. Park, *Water Res*., 2005, **39**, 533.

26 L.J. Yu, S.S. Shukla, L.D. Kenneth, A. Shukla and J.L. Margrave, *J. Hazard. Mater. B*., 2003, **100**, 53.

27 V.K. Gupta and S. Sharma, *Environ. Sci. Technol*., 2002, **36**, 3612.

28 B. Liu and Y.M. Huang, *J. Mater. Chem*., 2011, **21**, 17413.

29 M.S. Mauter and M. Elimelech, *Environ. Sci. Technol*., 2008, **42**, 5843.

30 J.P. Ruparelia, S.P. Duttagupta, A.K. Chatterjee and S. Mukherji, *Desalination*., 2008, **232**, 145.

31 J.H. Zhu, H.b. Gu, J. Guo,M.J. Chen, H.G. Wei, Z.P. Luo and H.A. Colorado, et al. *J. Mater. Chem. A*., 2014, **2**, 2256.

32 H.L. Ma, Y.Z. Zhang, Q.H. Hu, D. Yan, Z.Z. Yu and M.L. Zhai, *J. Mater. Chem.*, 2012, **22**, 5914.

33 C.J. Madadrang, H.Y. Kim, G.H. Gao, N. Wang, J. Zhu, H. Feng, M. Gorring, M. L. Kasner,

and S.F. Hou, *Appl. Mater. Interfaces*., 2012, **4**, 1186.

34 Z.H .Huang, X.Y. Zheng, W. Lv, M. Wang, Q.H. Yang and F.Y Kang, *Langmuir.*, 2011, **27**, 7558.

35 V. Chandra and K.S. Kim, *Chem. Commun.,* 2011, **47**, 3942.

36 V. Chandra, J. Park, Y. Chun, J.W. Lee, I-C. Hwang, and K.S. Kim, *ACS Nano*., 2010, **47**, 3979.

37 G.X. Zhao, J.X. Li, X.M. Ren, C.L. Chen and X.K. Wang, *Environ. Sci. Technol*., 2011, **45**, 10454.

38 Y. Gao, Y. Li, L. Zhang, H. Huang, J.J. Hua and H Huang, et al. *J Colloid Interface Sci*., 2012, **368**, 540.

39 Y. Sun, Q. Wang, C. Chen, X. Tan and X. Wang, *Environ. Sci. Technol*., 2012, **46**, 6020.

40 S.T. Yang, S. Chen, Y. Chang, A. Cao, Y. Liu and H. Wang, *J. Colloid .Interface Sci.*, 2011, **359**, 24.

41 D.R. Dreyer, S. Park, C.W. Bielawski and R.S. Ruoff, *Chem. Soc. Rev*., 2010, **39**, 228.

42 T.S. Sreeprasad, S.M. Maliyekkal, K.P. Lisha and T. Pradeep, *J. Hazard. Mater.*, 2011, **186**, 921.

43 T. Zhang, Z.G. Cheng, Y.B. Wang, Z.J. Li, C.X. Wang, Y.B. Li and Y. Fang, *Nano Lett.*, 2010, **10**, 4738.

44 X.J. Deng, L.L. Lu, H.W. Li and F. Luo, *J. Hazard. Mater*., 2010, **183**, 923.

45 S.T. Yang, Y.L. Chang, H.F. Wang, G.B. Liu, S.Chen, Y.W. Wang, Y.F. Liu and A.N. Cao, *J. Colloid. Interface Sci*., 2010, **351**, 122.

46 C. Petit, C. Mendoza and T.J. Bandosz, *Langmuir*., 2010, **26**, 15302.

47 R. Zacharia, H. Ulbricht and T. Hertel, *Phys. Rev. B.,* 2004, **69**, 155406.

48 Z. Wu, D. Wang, W. Ren, J. Zhao, G. Zhou, F. Li and H. Cheng, *Adv. Funct. Mater*., 2010, **20**, 3595.

49 H.M. Sun, L.Y. Cao and L.H. Lu, *Nano Res.,* 2011, **46**, 550.

50 M. Amara and H. Kerdjoudj, *Desalination*., 2004, **168**, 195.

51 M. Ghoul, M. Bacquet and M. Morcellet, *Water Res*., 2003,**37** ,729.

52 J.H. Zhu, S.Y. Wei, H.B. Gu, Sowjanya. B. Rapole, Q. Wang, Z.P. Luo, Neel Haldolaarachchige, D.P. Young, and Z.H. Guo, *Environ. Sci. Technol*., 2012, **46**, 977.

53 W.S. Hummers and R.E. Offeman, *J. Am. Chem. Soc*., 1958, **80**, 1339.

54 S. Bai, X.P. Shen, X. Zhong, Y. Liu, G.X. Zhu, X. Xu and K.M. Chen, *Carbon*., 2012, **50**, 2337.

55 S.H. Huang and D.W. Chen, *J. Hazard. Mater*., 2009, **163**, 174.

56 G. Bayramo˘glu and M.Y. Arıca, *Sep. Purif. Technol*., 2005, **45**, 192.

57 Y.G. Zhao, H.Y. Shen, S.D. Pan and M.Q. Hu, *J. Hazard. Mater*., 2010, **182**, 295.

58 J. Fang, Z. Gu, D. Gang, C. Liu, E.S. Ilton and B. Deng, *Environ. Sci. Technol.,* 2007, **41**, 4748.

59 L.L. Li, L.L. Fan, M. Sun, H.M. Qiu, X.J. Li, H.M. Duan and C.N. Luo, *Colloids Surf B Biointerfaces.*, 2013, **107**, 76.

60 S. Asuha, X.G. Zhou and S. Zhao, *J. Hazard. Mater*., 2010, **181**, 204.

61 W.T. Yu, L.Y. Zhang, H.Y. Wang and L.Y. Chai, *J. Hazard. Mater*., 2013, **260,** 789.

62 M. Bhaumik, A. Maity, V.V. Srinivasu and M.S. Onyango, *J. Hazard. Mater*., 2011, **190**, 381.

63 S.C. Wei, D.T. Li, Z. Huang, Y.Q. Huang and F. Wang, *Bioresour. Technol.,* 2013, **134**, 407.

64 C.S. Shen, H. Chen, S.S. Wu, Y.Z. Wen, L.N. Li , Z. Jiang, M.C. Li and W.P. Liu, *J. Hazard. Mater*., 2013, **244**, 689-

65 H.J. Gao, Y. Wang and L.Q. Zheng, *J. Environ. Manage*., 2014, **137**, 81.

66 D. Park, Y.S. Yun, H.W. Lee and J.M. Park, *Bioresour. Technol*., 2008, **99**, 1141.

Tables

Table 1. Thermodynamic parameters at different temperatures. (Cr(VI) ions concentration 90 $mg.L^{-1}$, adsorbent dosage 0.1 $g.L^{-1}$, pH 2.0, stirring speed 120 rpm, contact time 24 h.**)**

Adsorbent	T/K	ΔG($kJ.mol^{-1}$)	ΔH($kJ. mol^{-1}$)	ΔS($J\ mol^{-1}. k^{-1}$)
4PEI-GO	298	-3.83	9.28	43.83
	308	-4.27		
	318	-4.71		
	328	-5.15		

Table 2. Adsorption capacities of various adsorbents for Cr(VI).

Adsorbent	Optimum pH	q_{max} ($mg.g^{-1}$)	Reference
Ethylenediamine-functionalized Fe_3O_4	2.5	61.35	[57]
PVP modified activated carbon	2.25	53.7	[58]
Graphene oxide functionalized with magnetic cyclodextrin–chitosan	3.0	67.66	[59]
Mesoporous TiO_2	3.0	33.9	[60]
Synthetic poly(m-phenylenediamine)	2.0	500	[61]
Polypyrrole/Fe_3O_4 nanocomposite	2.0	169.4	[62]
Hierarchical porous carbon	2.0	398.40	[63]
Chitosan–Fe(III) complex	5.0	173.1	[64]
Ionic liquid-based cross-linked polymer	5.6	391.4	[65]
Polyethyleneimine modified graphene oxide	2.0	539.53	This work

Table 3. Results and Parameters Associated with Langmuir and Freundlich Models for Cr(VI) on 4PEI-GO. (initial concentration 10−400 $mg.L^{-1}$, adsorbent dosage 0.1 $g.L^{-1}$, pH 2.0, temperature 298 K, stirring speed 120 rpm, contact time 24 h.)

Isotherm type	**isotherm constants**	
Langmuir	k_l($L\ mg^{-1}$)	0.036
	q_{cal}($mg\ g^{-1}$)	581
	q_{exp}($mg\ g^{-1}$)	539.53
Freundlich	k_f($mg\ g^{-1}\ (mg\ L^{-1})^n$)	134.41
	n	4.16

Table 4. Parameters of a peudo-second-order Kinetic Model Fitting Cr(VI) Adsorption Kinetics. (Cr(VI) ions concentration 90 mg.L^{-1}, adsorbent dosage 0.1 g.L^{-1}, pH 2.0, temperature 298 K, stirring speed 120 rpm, contact time 24 h.**)**

adsorbent	q_{exp}(mg g^{-1})	q_{cal}(mg g^{-1})	v_o(mg $g^{-1}min^{-1}$)	k_2(mL mg^{-1} min^{-1})	R^2
4PEI-GO	318.05	320.51	23.62	$2.3x10^{-4}$	0.999

Table 5. The concentration of Cr(VI) in electroplating wastewater and the removal (%) after treating 100 mL of electroplating wastewater with 0.01 g.L^{-1} 4PEI-GO adsorbent. (temperature 298 K, stirring speed 120 rpm, contact time 24 h, Remove efficiency±S.D.**)**

Matrix	pH	C_o(mg L^{-1})	C_e(mg L^{-1})	Removal (%)
wastewater	2.0	10.963±0.038	0.402±0.026	96.35±0.06

Legends of Figures

Fig.1. Effect of the content of the PEI on adsorption capacity: Cr(VI) ions concentration 76 $mg.L^{-1}$, adsorbent dosage 0.1 $g.L^{-1}$, temperature 298 K, stirring speed 120 rpm, contact time 24 h.

Fig.2. FT-IR images of: (a) the GO, (b) the 4PEI-GO.

Fig.3. (a) SEM image of the GO, (b) SEM image of the 4PEI-GO, (c) SEM image of the 4PEI–GO after adsorption of Cr(VI).

Fig.4. Effects of solution pH on adsorption capacity: Cr(VI) ions concentration 90 $mg.L^{-1}$, adsorbent dosage 0.1 $g.L^{-1}$, temperature 298 K, stirring speed 120 rpm, contact time 24 h.

Fig.5. Effects of temperature on adsorption capacity: Cr(VI) ions concentration 90 $mg.L^{-1}$, adsorbent dosage 0.1 $g.L^{-1}$, pH 2.0, Stirring speed 120 rpm, contact time 24 h.

Fig.6. Linear plot of ln (q_e/c_e) vs 1000/T for the adsorption of Cr(VI) on 4PEI-GO, (Cr(VI) ions concentration 90 $mg.L^{-1}$. adsorbent dosage 0.1 $g.L^{-1}$, pH 2.0, stirring speed 120 rpm, contact time 24 h)

Fig.7. Adsorption isotherms of Cr(VI) on the 4PEI-GO at pH 2.0. (initial concentration 10−400 $mg.L^{-1}$, adsorbent dosage 0.1 $g.L^{-1}$, pH 2.0, temperature 298 K, stirring speed 120 rpm, contact time 24 h.)

Fig.8. (a) The Langmuir isotherm, (b) the Freundlich isotherm.

Fig.9. Energy dispersive X-ray (EDX) analysis of: (a) Cr(VI) ions loaded GO, (b) Cr(VI) ions loaded 4PEI-GO.

Fig.10. Effects of reaction time on adsorption capacity: Cr(VI) ions concentration 90 $mg.L^{-1}$, adsorbent dosage 0.1 $g.L^{-1}$, temperature 298 K, pH 2.0, stirring speed 120 rpm, contact time 24 h.

Fig.11. The pseudo-second-order kinetics

Fig.12 The effects of coexisting metal ions on Cr(VI) adsorption.

Fig.13 Cr 2p spectrum of the Cr-laden 4PEI-GO.

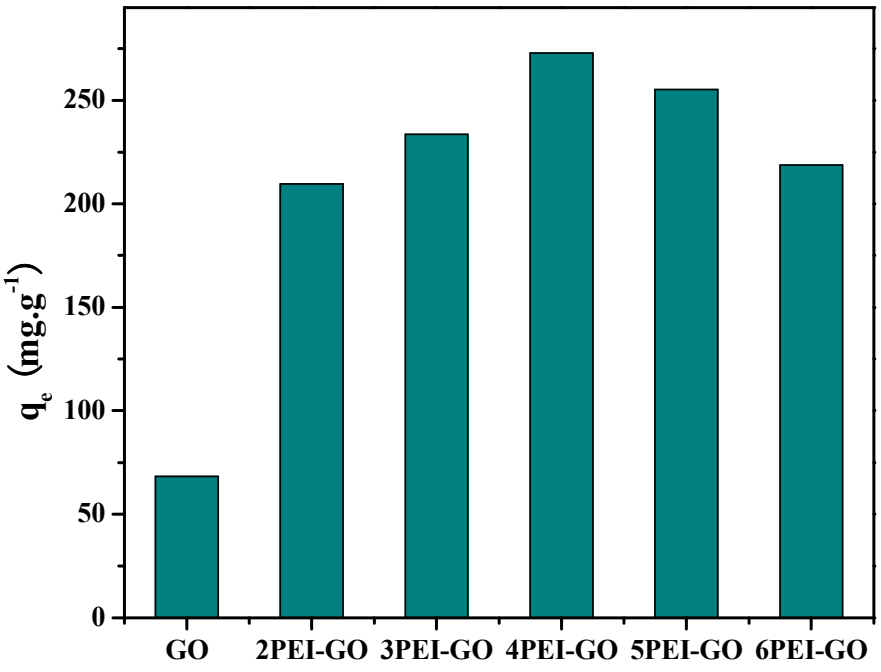

Fig. 1

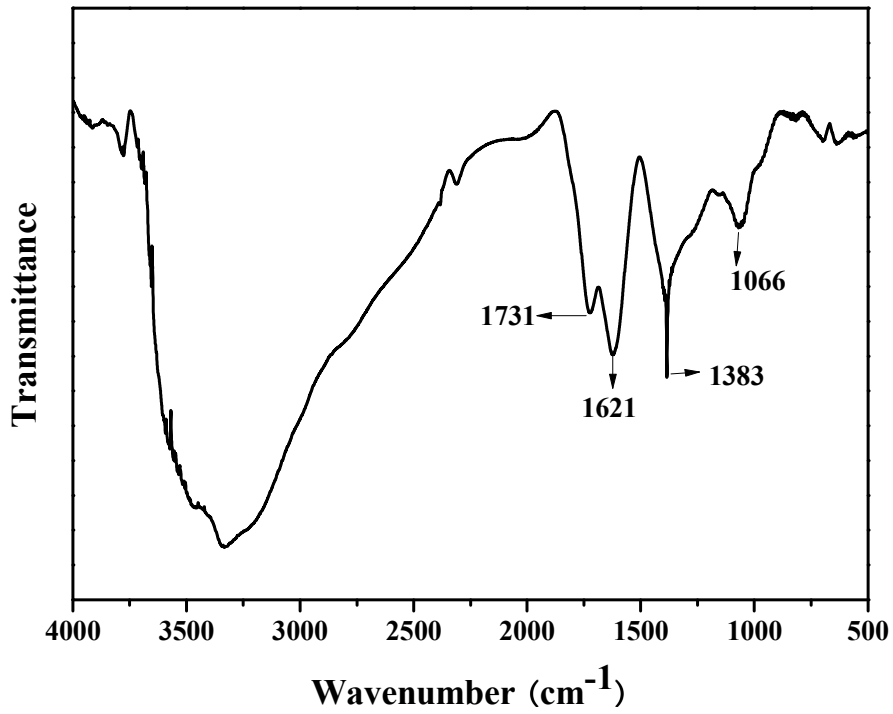

Fig. 2a

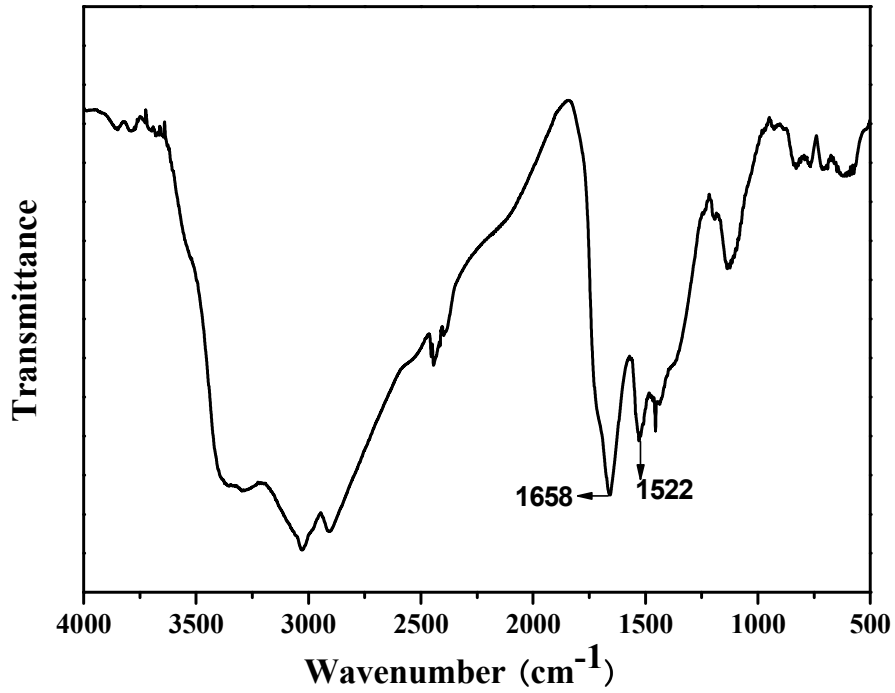

Fig. 2b

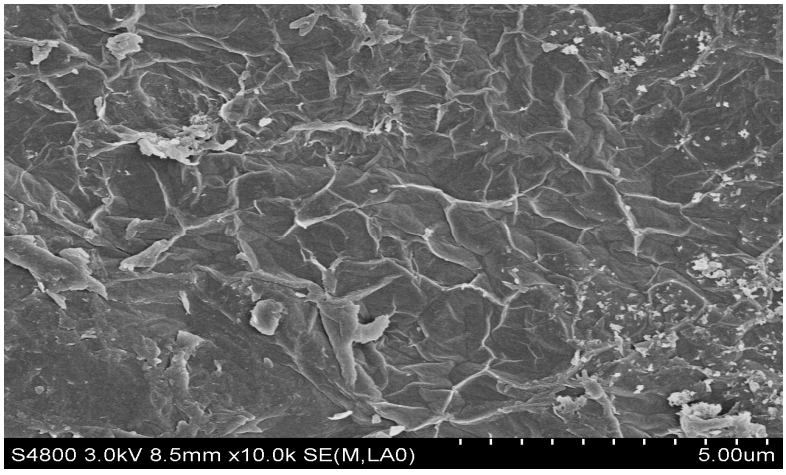

Fig. 3a

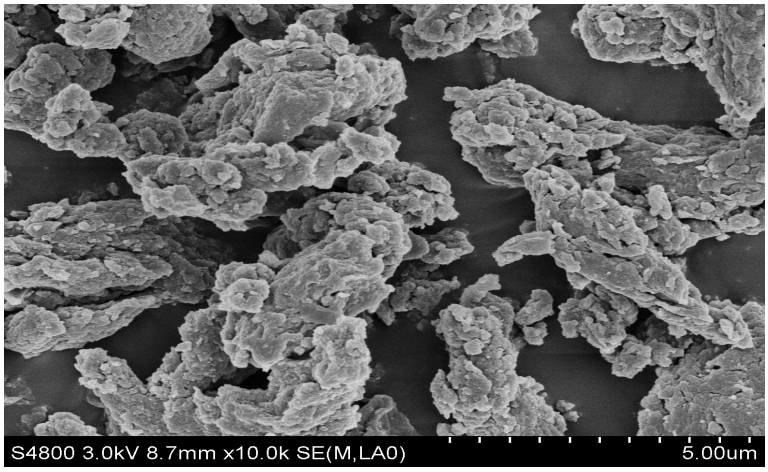

Fig. 3b

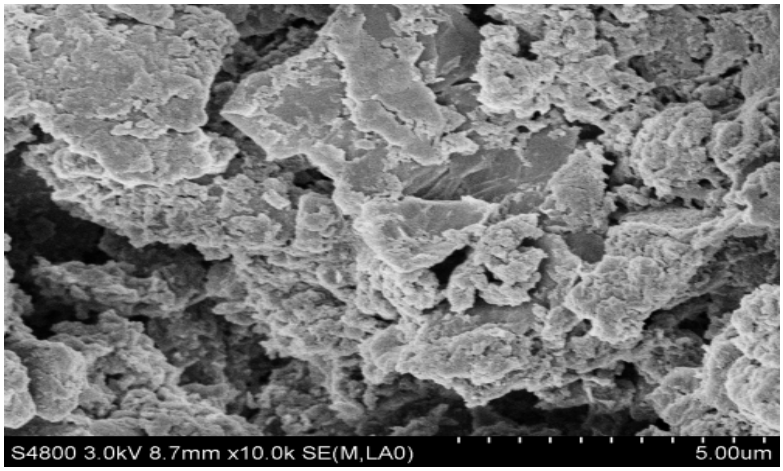

Fig. 3c

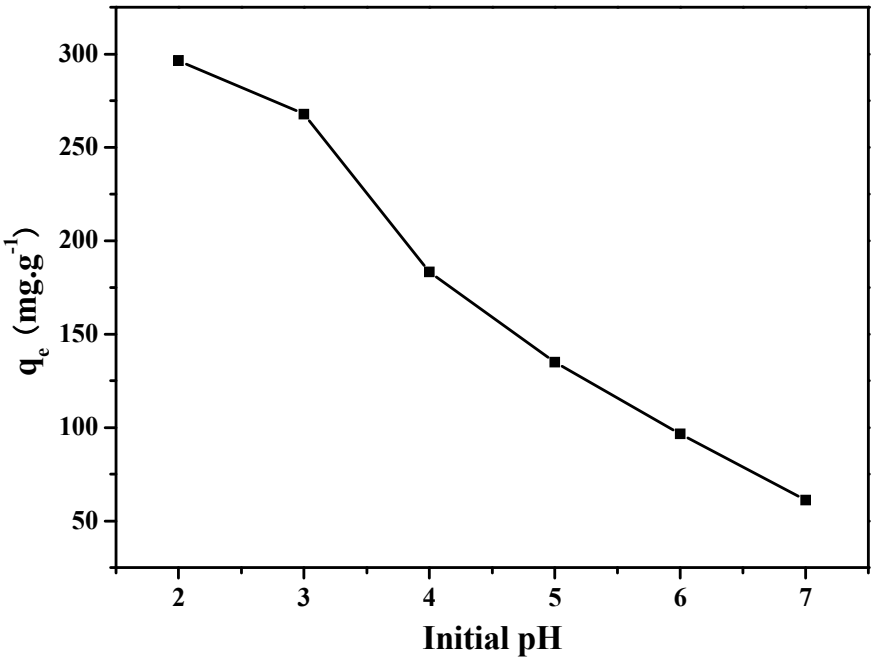

Fig. 4

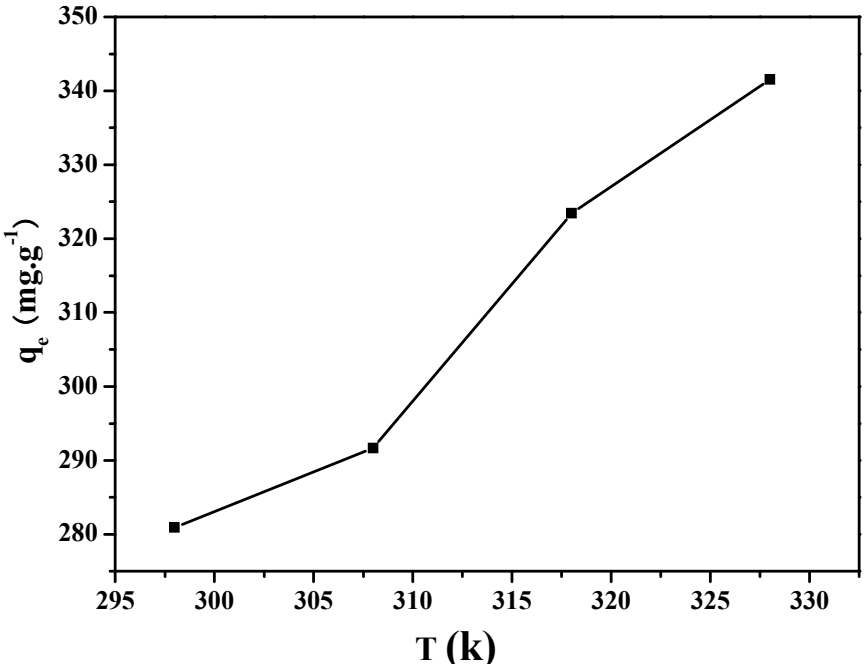

Fig. 5

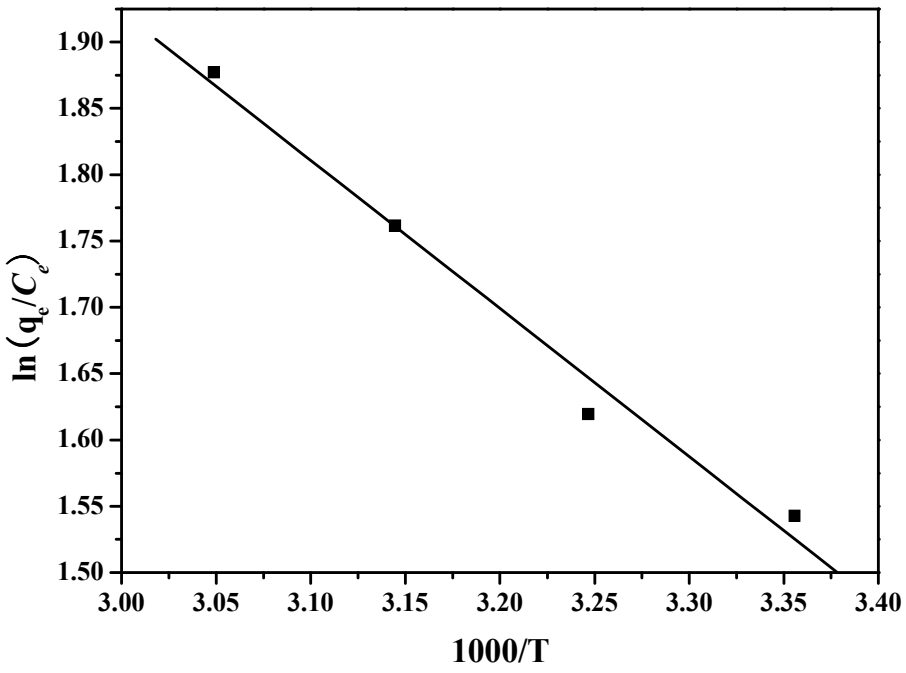

Fig. 6

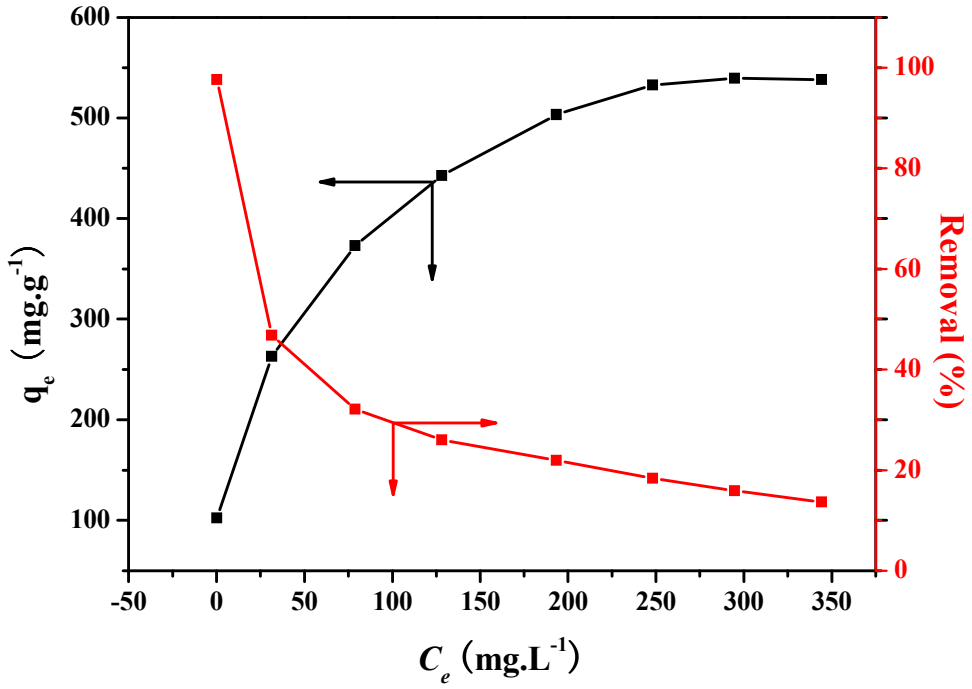

Fig. 7

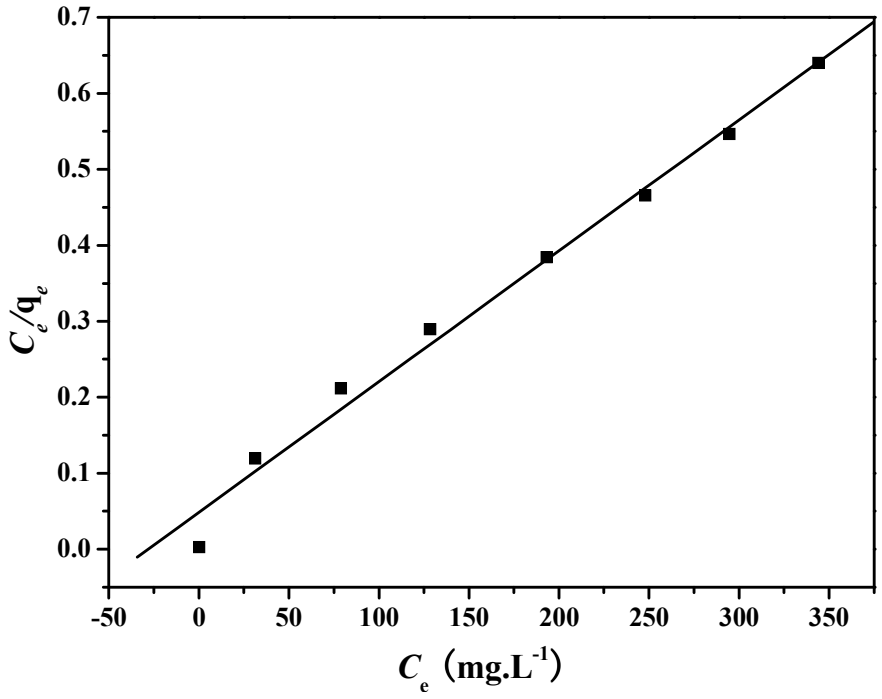

Fig. 8a

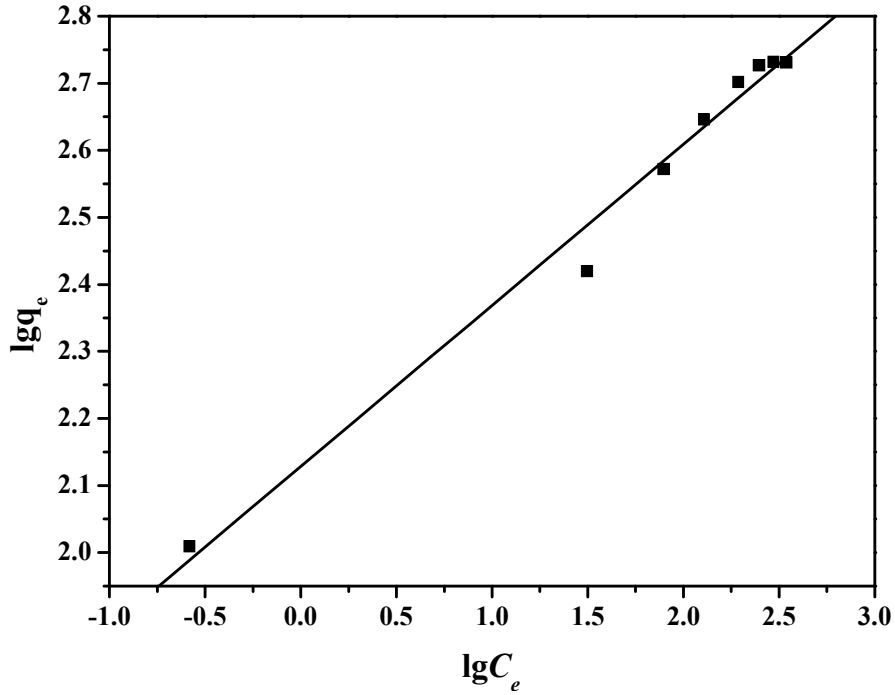

Fig. 8b

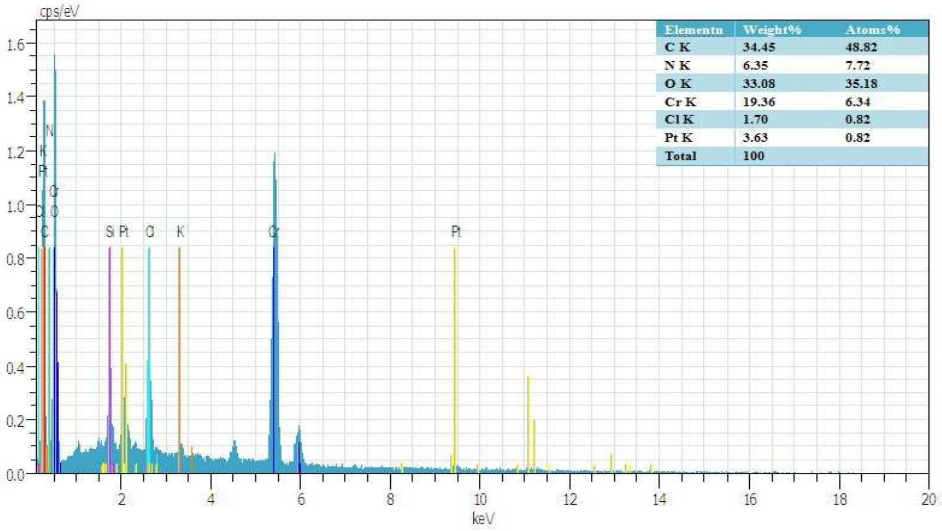

Fig. 9a

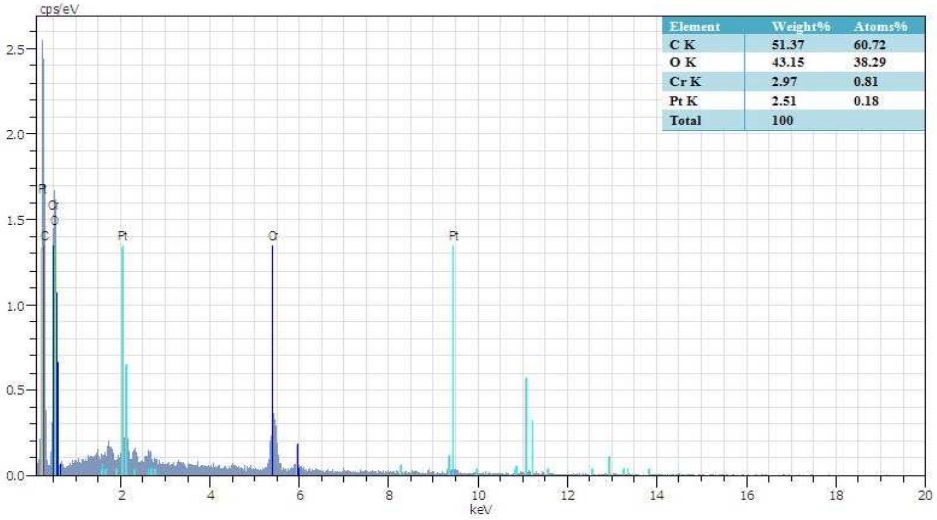

Fig. 9b

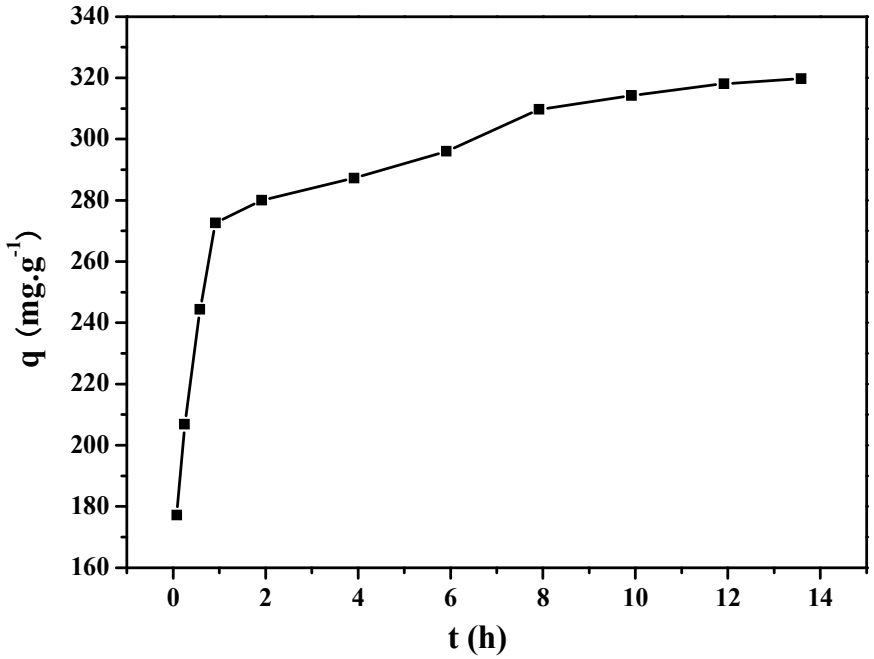

Fig. 10

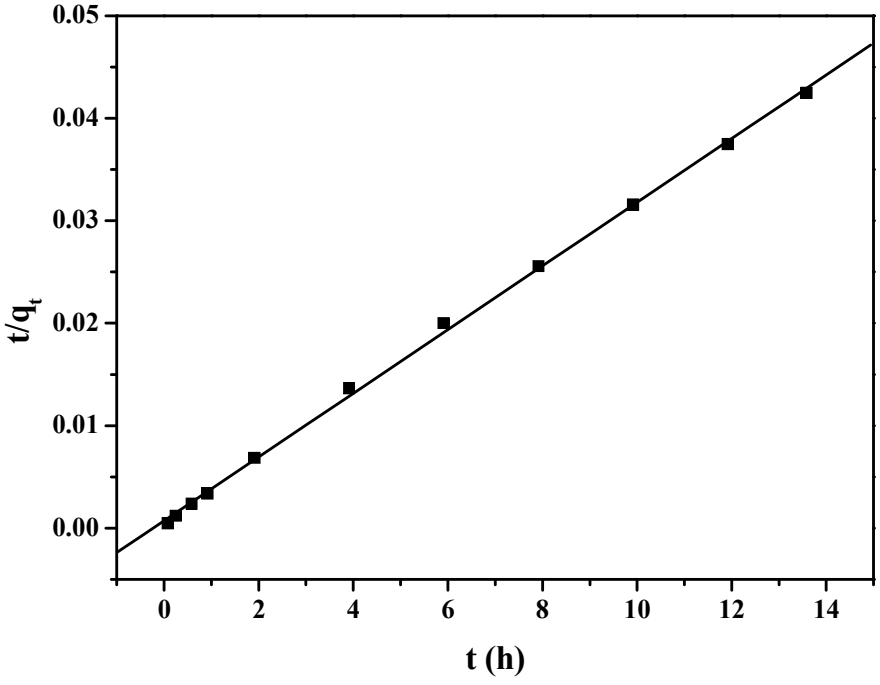

Fig. 11

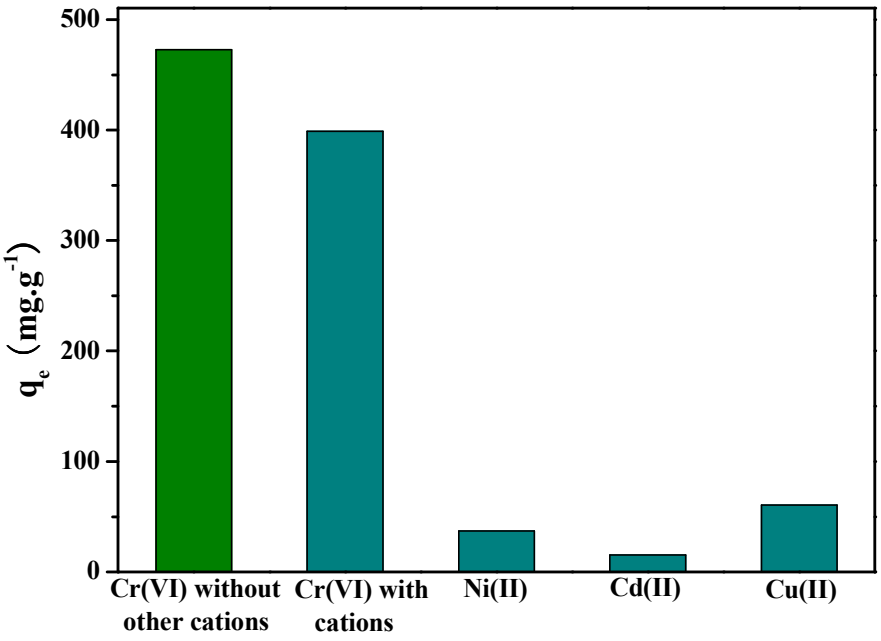

Fig. 12

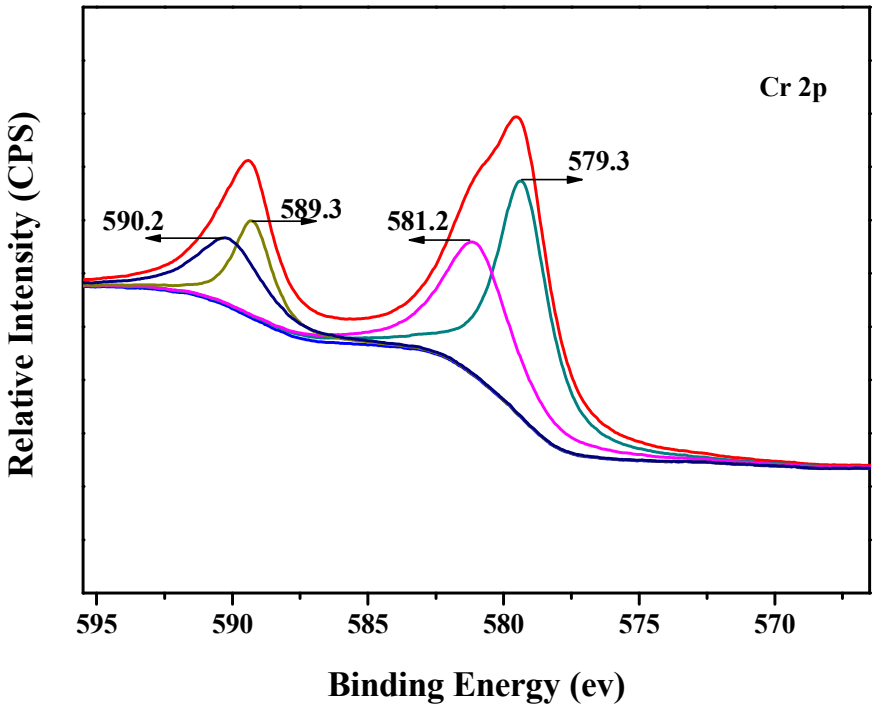

Fig. 13